Cellular Microbiology (2016) **18**(1), 137–147
doi:10.1111/cmi.12492
First published online 3 September 2015

Macrophages recognize the *Helicobacter pylori* type IV secretion system in the absence of toll-like receptor signalling†

Manuel Koch, Hans-Joachim Mollenkopf and Thomas F. Meyer*
Department of Molecular Biology, Max Planck Institute for Infection Biology, Charitéplatz 1, 10117 Berlin, Germany.

Summary

Helicobacter pylori **strains carrying the cag pathogenicity island (cagPAI) provoke an increased inflammatory response, conferring an increased risk of ulcer formation and carcinogenesis. How the immune system recognizes the presence of cagPAI positive strains is yet unclear. By comparing the transcriptional response of wild type and MyD88/Trif$^{-/-}$ bone marrow macrophages to infection with *H. pylori*, we found that the majority of regulated genes were dependent on toll-like receptor (TLR) signalling. To determine the role of TLR-independent responses, we analysed the transcriptome of MyD88/Trif$^{-/-}$ bone marrow macrophages at different time points after infection with cagPAI positive versus negative strains. We identified a group of genes that exhibited different kinetic behaviour depending on whether cagPAI was present. Analysis of their gene expression kinetics demonstrated that this responsiveness to cagPAI was observed only in MyD88/Trif$^{-/-}$ macrophages. This group of cagPAI-sensing genes was enriched for AU-rich element containing early response genes involved in immune regulation, including interleukin-1β (IL-1β) and tumor necrosis factor-α (TNF-α). Recognition of cagPAI positive strains was found to be mediated by the type IV secretion system (cagT4SS), rather than its effector protein CagA. We hypothesize that anergic macrophages of the gastric mucosa initiate an innate immune response following detection of the T4SS of *H. pylori*.**

Received 7 July, 2015; revised 14 July, 2015; accepted 17 July, 2015. *For correspondence. E-mail tfm@mpiib-berlin.mpg.de; Tel. (+49)-30-28-460-400; Fax (+49)-30-28-460-401.
†Microarray data presented in this paper have been deposited in the National Center for Biotechnology Information Gene Expression Omnibus (GEO; http://www.ncbi.nlm.nih.gov/geo/) and are accessible through GEO series accession number GSE56791.

Introduction

Helicobacter pylori is a Gram-negative bacterium colonizing the stomach of ~50% of the world's population. Infection with *H. pylori* usually occurs during childhood and persists life-long if untreated. It may lead to gastritis, peptic ulcer disease and gastric mucosa-associated lymphatic tissue lymphoma or gastric adenocarcinoma. A pronounced immune response and severe long-term consequences are mainly associated with strains carrying the cagPAI, which encodes a cagT4SS and its only known effector protein, CagA (Kusters *et al.*, 2006). The mechanism by which the innate immune system other than epithelial cells is alerted to the presence of cagPAI positive strains has received almost no attention so far. It is likely to have significant implications, however, especially in light of the emerging beneficial effects of *H. pylori* infection *per se*, such as protection against asthma and inflammatory bowel disease (Oertli *et al.*, 2012; Engler *et al.*, 2015), as well as the increasing appreciation of the microbiota in health and disease.

The concentration of bacteria housed in the gastrointestinal tract ranges from 10^2 per milliliter in the stomach to 10^{11} per milliliter in the colon (Walter and Ley, 2011). It is thus bombarded with ligands that may interact with members of the TLR family and trigger an innate immune response, regardless of whether they are derived from a commensal or pathogenic bacterium. However, an important task of the immune system consists of discriminating between normal microbiota and virulent pathogens. This may be one reason why the resident innate immune cells of the gastrointestinal tract, such as the lamina propria dendritic cells or macrophages, show anergy towards ligands that trigger a TLR response and possibly also other innate receptors such as NOD1 and NOD2 (Mowat and Bain, 2011; Smythies *et al.*, 2010).

Secretion systems such as T3SS and T4SS are critical determinants of the pathogenic potential of Gram-negative bacterial isolates or species, e.g. in *Bordetella pertussis* or *Bartonella henselae* harbouring a T4SS, or in enteropathogenic *Escherichia coli* exhibiting a T3SS. A fine-tuned innate response against these structures or translocated effectors could thus facilitate mounting a balanced defence against potential invaders. Specific recognition of cagPAI positive *H. pylori* followed by secretion of pro-inflammatory cytokines would favour the infiltration of inflammatory cells such as monocytes and neutrophils that dominate the inflammatory response.

In monocyte-derived cells of the bone marrow, recognition of *H. pylori* occurs via TLRs such as TLR2, TLR4 and TLR9 (Rad *et al.*, 2009). However, cagPAI positive and negative strains express similar amounts of TLR ligands, yet several lines of evidence show that the innate immune system mounts a stronger response to positive strains. Both mice and humans have much higher inflammatory scores during infection with cagPAI positive strains (Yamaoka *et al.*, 1997; Arnold *et al.*, 2011). Mice can also be colonized more easily with cagPAI negative strains, and only one mouse-adapted strain established so far maintains expression of a functional cagPAI *in vivo* for at least 1 month before it is lost (Arnold *et al.*, 2011). Gastric epithelial cell lines such as AGS cells, which lack specific TLR-dependent pathways (Belogolova *et al.*, 2013), are able to differentiate between cagPAI positive and negative *H. pylori in vitro* depending on the cagT4SS (Bartfeld *et al.*, 2010). This strongly suggests that TLR-independent mechanisms are involved in recognizing cagPAI positive strains.

To illuminate the open issue of mucosal recognition, we used wild type and MyD88/Trif$^{-/-}$ bone marrow-derived macrophages (BMMs), which lack the adaptor proteins of all TLRs and are thus unresponsive to TLR signalling (Kawai and Akira, 2011). We have previously shown that T4SS-induced up-regulation of miR-155 in these cells is independent of NOD1 or NOD2 (Koch *et al.*, 2012). Here, we analysed global gene expression and kinetics in wild type and MyD88/Trif$^{-/-}$ macrophages infected with cagPAI positive and negative strains. We found that anergic but not wt macrophages recognize the presence of the T4SS and respond via altered kinetics of a subset of genes that includes a prominent set of pro-inflammatory genes with AU-rich elements (AREs).

Results

Toll-like receptor-dependent and independent effects of Helicobacter pylori *on BMMs*

We compared the gene expression profiles of *H. pylori* P12-infected [3 h, multiplicity of infection (MOI) 50] BMMs from wt and MyD88/Trif$^{-/-}$ mice by microarray analysis. A large number of genes were up-regulated upon infection in both. To analyse and focus on the key genes, those with >10-fold up-regulation in wt BMMs upon *H. pylori* infection (normalized to mock) were investigated for subsequent analyses. As expected, the majority of these regulated genes (96 of 136) were regulated more strongly (at least 1.5-fold) in wt BMMs (Supporting Information Fig. 1A), suggesting some degree of TLR-dependence. The remaining 40 genes, however, were regulated equally (<1.5-fold difference) or more strongly in MyD88/Trif$^{-/-}$ BMMs and were thus categorized as TLR-independent (Supporting Information Fig. 1B).

The cagPAI induces changes in kinetics of ARE-containing genes in MyD88/Trif$^{-/-}$ BMMs

Because *H. pylori*-induced innate signalling in epithelial cells strongly depends on the presence of cagPAI (Backert and Naumann, 2010; Belogolova *et al.*, 2013), we carried out a further microarray analysis using infection with wt P12 as well as an isogenic cagPAI deletion mutant (P12Δ*cagPAI*) (MOI 50). We used MyD88/Trif$^{-/-}$ BMMs to investigate this process in order to focus on the TLR-independent responses. Because induction of pro-inflammatory genes occurs in distinct waves with different kinetics (Hao and Baltimore, 2009), analysis was carried out at 1 and 3 h post-infection (p.i.). Of the 543 genes significantly up-regulated at 1 h p.i., 365 were more strongly and none less strongly up-regulated after infection with P12 compared to P12Δ*cagPAI*. Surprisingly, at 3 h p.i., only nine of these remained more strongly up-regulated with P12, whereas 74 genes were now more strongly up-regulated in P12Δ*cagPAI*. When analysing these 74 genes in more detail, we noticed that many of them were known early or intermediate response genes of the inflammatory cascade (Hao and Baltimore, 2009), whose stability is regulated by the presence of pentameric AREs in the 3´UTR. Using the ARESite algorithm (Gruber *et al.*, 2011), we confirmed that of these 74 genes, 59 did indeed contain AREs (four genes were not in the database, Table 1). Compared to ~45% of pentameric ARE positive genes in the whole genome (ARESite: 11 056 out of 23 184, Ensembl release 2012), this represents a highly significant enrichment (χ^2-test $p < 0.0001$; odds ratio: 5.884, 95% CI: 3.089 to 11.210). Of the 17 genes that regulated more than twofold in all conditions, all contained at least one, and 15 contained multiple AREs. Genes containing many ARE pentamers in their 3´UTR share two main features: early onset of expression upon a stimulus ('early response genes') and a fast mRNA decay (Hao and Baltimore, 2009; Schwanhausser *et al.*, 2011).

Table 1. Genes up-regulated more strongly at 3 h p.i. in MyD88/Trif$^{-/-}$ BMMs in response to P12Δ*cagPAI* compared to wt P12. Inclusion criteria were >1.5-fold induction by P12 compared to mock at 60 min p.i., >1.5-fold stronger up-regulation in response to P12 compared to P12Δ*cagPAI* at 60 min p.i. and >1.5-fold stronger in response to P12Δ*cagPAI* compared to P12 at 3 h p.i.. The number of pentameric AU-rich elements in the 3´ UTR was determined according to ARESite Gruber *et al.* (2011).

Gene name	Accession no.	ARE pentamer	P12/P12Δ*cagPAI* 3 h	P12/P12Δ*cagPAI* 60 min	P12/mock 60 min
Egr1	NM_007913	2	−8.37	25.72	24.95
Il1a	NM_010554	3	−4.55	11.83	31.57
Fos	NM_010234	4	−3.87	8.50	13.05
Jmjd3	NM_001017426	3	−3.76	5.67	5.44
Nr4a1	NM_010444	3	−3.30	3.83	3.83
Tmem88	NM_025915	1	−3.20	8.22	8.70
Il1b	NM_008361	4	−3.18	10.20	20.77
Tnfsf9	NM_009404	2	−3.06	5.58	8.19
Egr2	NM_010118	3	−3.00	8.76	8.70
Slco4a1	NM_148933	1	−2.93	4.25	3.00
Spred2	NM_033523	2	−2.60	2.69	1.57
Ccrn4l	NM_009834	4	−2.55	7.25	6.09
Maff	NM_010755	4	−2.54	3.64	4.88
Socs3	NM_007707	4	−2.51	5.15	6.36
Csf2	NM_009969	9	−2.46	17.62	58.62
Edn1	NM_010104	3	−2.45	5.43	7.21
Kcnj10	NM_020269	4	−2.41	2.49	1.93
Rgs1	NM_015811	3	−2.35	1.72	2.09
Tnfaip3	NM_009397	5	−2.17	9.57	12.40
Dusp4	NM_176933	2	−2.02	2.26	2.41
Ptgs1	NM_008969	0	−2.02	1.82	1.89
Klf2	NM_008452	1	−1.97	3.65	3.22
F3	NM_010171	7	−1.94	4.34	8.43
Spry1	NM_011896	2	−1.91	4.15	5.05
Trib1	NM_144549	0	−1.91	4.34	5.48
Mcl1	NM_008562	8	−1.90	2.78	3.22
Hivep2	NM_010437	3	−1.89	3.16	2.44
Atp10d	NM_153389	5	−1.85	2.14	1.92
Ube2d1	NM_145420	1	−1.84	2.54	2.49
Rnf19a	NM_013923	3	−1.83	1.92	2.25
Dnajb4	NM_025926	3	−1.82	1.82	2.62
Fbxl11	NM_001001984	3	−1.81	2.40	1.77
Nfe2l2	NM_010902	1	−1.81	2.60	2.34
Hspa1a	NM_010479	1	−1.80	4.69	7.25
Errfi1	NM_133753	4	−1.79	4.78	6.46
Cd83	NM_009856	2	−1.78	3.51	4.97
B630005N14Rik	NM_175312	n.d.	−1.76	2.14	2.06
Phlda1	NM_009344	3	−1.75	9.06	8.73
Ier2	NM_010499	n.d.	−1.75	3.37	4.53
AY078069	NM_172142	1	−1.72	3.72	2.63
Dusp6	NM_026268	1	−1.72	1.71	1.79
Gdf15	NM_011819	5	−1.71	2.16	2.24
St6gal1	NM_145933	1	−1.70	1.90	1.79
Rps6ka5	NM_153587	5	−1.69	1.94	1.84
Sepn1	NM_029100	0	−1.69	2.69	2.19
Itpr1	NM_010585	5	−1.68	2.60	2.20
Smyd3	NM_027188	1	−1.68	1.90	2.34
Snag1	NM_130796	7	−1.67	1.96	2.30
Gpr84	NM_030720	1	−1.67	2.13	1.97
Mia1	NM_019394	0	−1.66	2.05	2.84
Tnf	NM_013693	8	−1.65	3.21	3.93
Synj2	NM_011523	7	−1.65	2.01	1.97
Eif2ak4	NM_013719	1	−1.65	1.77	1.76
Itga5	NM_010577	2	−1.63	2.85	2.24
Mamdc2	NM_174857	1	−1.63	1.71	2.06
Cited2	NM_010828	0	−1.63	3.09	2.57
Ddit4	NM_029083	0	−1.63	2.77	2.94
Btg2	NM_007570	5	−1.60	3.29	4.27
Eid3	NM_025499	n.d.	−1.59	3.02	2.62
Id2	NM_010496	3	−1.57	1.84	2.15
Myc	NM_010849	2	−1.57	5.25	4.60
AI428795	NM_024477	n.d.	−1.57	4.06	2.54

(Continues)

Table 1 *(Continued)*

Gene name	Accession no.	ARE pentamer	P12/P12Δ*cagPAI* 3 h	P12/P12Δ*cagPAI* 60 min	P12/mock 60 min
Stil	NM_009185	0	−1.56	1.68	2.06
Phr1	NM_207215	4	−1.55	2.63	1.89
Rasgef1b	NM_181318	2	−1.55	4.12	4.55
Lox	NM_010728	0	−1.55	2.56	3.53
Rtn1	NM_153457	0	−1.55	2.54	1.90
Nlrp3	NM_145827	5	−1.54	1.67	1.89
Sec61a2	NM_021305	2	−1.53	1.67	1.94
Adamts1	NM_009621	5	−1.52	3.31	3.48
Farp2	NM_145519	0	−1.52	1.66	1.71
Mt1	NM_013602	0	−1.52	1.58	1.58
Nfkbiz	NM_030612	4	−1.50	9.55	11.23
Ccrl2	NM_017466	2	−1.50	3.01	4.54

Only MyD88/Trif$^{-/-}$ BMMs show cagPAI-sensitivity in their early response kinetics

For wt BMMs, Hao and Baltimore (2009) defined three groups of mRNAs that exhibit different kinetics upon stimulation with inflammatory stimuli such as lipopolysaccharide (LPS) and TNF-α: early (with a very rapid onset and decay), intermediate (with slightly later onset and slower decay) and late (with a slow onset and high stability). We thus further validated our microarray data by performing time course analyses in wt and MyD88/Trif$^{-/-}$ BMMs for each class of genes from Table 1: we chose the ARE-containing genes TNFsf9, TNF-α and IL-1β, while the ARE-negative gene CCL-5 served as control. We infected wt and MyD88/Trif$^{-/-}$ BMMs with wt P12 and P12Δ*cagPAI* and performed time course analysis of gene expression by quantitative reverse transcription polymerase chain reaction (qRT-PCR). In wt BMMs, TNFsf9 showed early, TNF-α showed intermediate and IL-1β showed late response kinetics in response to infection with both strains (Fig. 1A–C). By contrast, in MyD88/Trif$^{-/-}$ BMMs, all three of these genes showed early response kinetics after infection with the cagPAI positive wt P12 *H. pylori*; after infection with P12Δ*cagPAI*, onset of expression was significantly delayed for all three ARE-containing genes (Fig. 1E–G). The maximum peak of IL-1β and TNFsf9 expression was also significantly lower during P12Δ*cagPAI* infection. CCL-5 on the other hand did not show a differential response to the two *H. pylori* strains at the time points tested (Fig. 1D and H). Thus, only MyD88/Trif$^{-/-}$ macrophages are able to differentiate between cagPAI positive and negative strains via different expression kinetics of ARE-containing genes.

To exclude that the observed effect could be due to different motilities of the two bacterial strains, we synchronized bacterial contact to MyD88/Trif$^{-/-}$ BMMs by centrifugation for 5 min prior to a 40 min infection time. In congruence with our results for the 1 h infection time point in Fig. 1 E–G, TNF-α, IL-1β and TNFsf9 were more strongly up-regulated in response to wt P12 than to P12Δ*cagPAI* (Supporting Information Fig. 2A–C). Thus, our results are not due to impaired motility of the P12Δ*cagPAI* deletion mutant.

To test whether the effect on the transcriptional level is also reflected on the protein level, we examined the expression of TNF-α and IL-1β by Western blot analyses. Figure 2 demonstrates that TNF-α expression on the protein level mimicked the observed RNA expression, being up-regulated at ~60 min p.i. and peaking at 90 min p.i. in the wt P12 infection in MyD88/Trif$^{-/-}$ BMMs (Fig. 2A), followed by a decline at 3 h p.i.. Up-regulation upon P12Δ*cagPAI* infection first occurred at 90 min p.i., peaking at 3 h p.i.. For both strains, levels remain slightly elevated as late as 5 h p.i.. Translation of IL-1β can be detected at ~90 min p.i. with wt P12 (Fig. 2B). By 3 h, both strains induced a similar up-regulation that was maintained until at least 5 h p.i.. Thus, for IL-1β and TNF-α, the early and stronger RNA up-regulation in response to wt P12 compared to P12Δ*cagPAI* infections is reflected on the protein level, whereas for IL-1β, the later time points in particular show evidence of increased protein stability, presumably due to higher complexity of posttranslational responses.

NOD1/NOD2 signalling is not required for detection of Helicobacter pylori *in macrophages*

The NOD-like receptor family members NOD1 and NOD2 are expressed in the cytosol of host cells and have been reported to recognize cagT4SS-translocated *H. pylori* peptidoglycan in epithelial cells (Viala *et al*., 2004; Chaput *et al*., 2006). To determine whether this is the effector involved in differentiation between cagPAI positive and negative *H. pylori*, we examined the function of Rip2, the adaptor protein of NOD1/2, in macrophages. We generated MyD88/Trif/Rip2$^{-/-}$ mice as described previously (Koch *et al*., 2012) and infected isolated BMMs with *H. pylori* P12

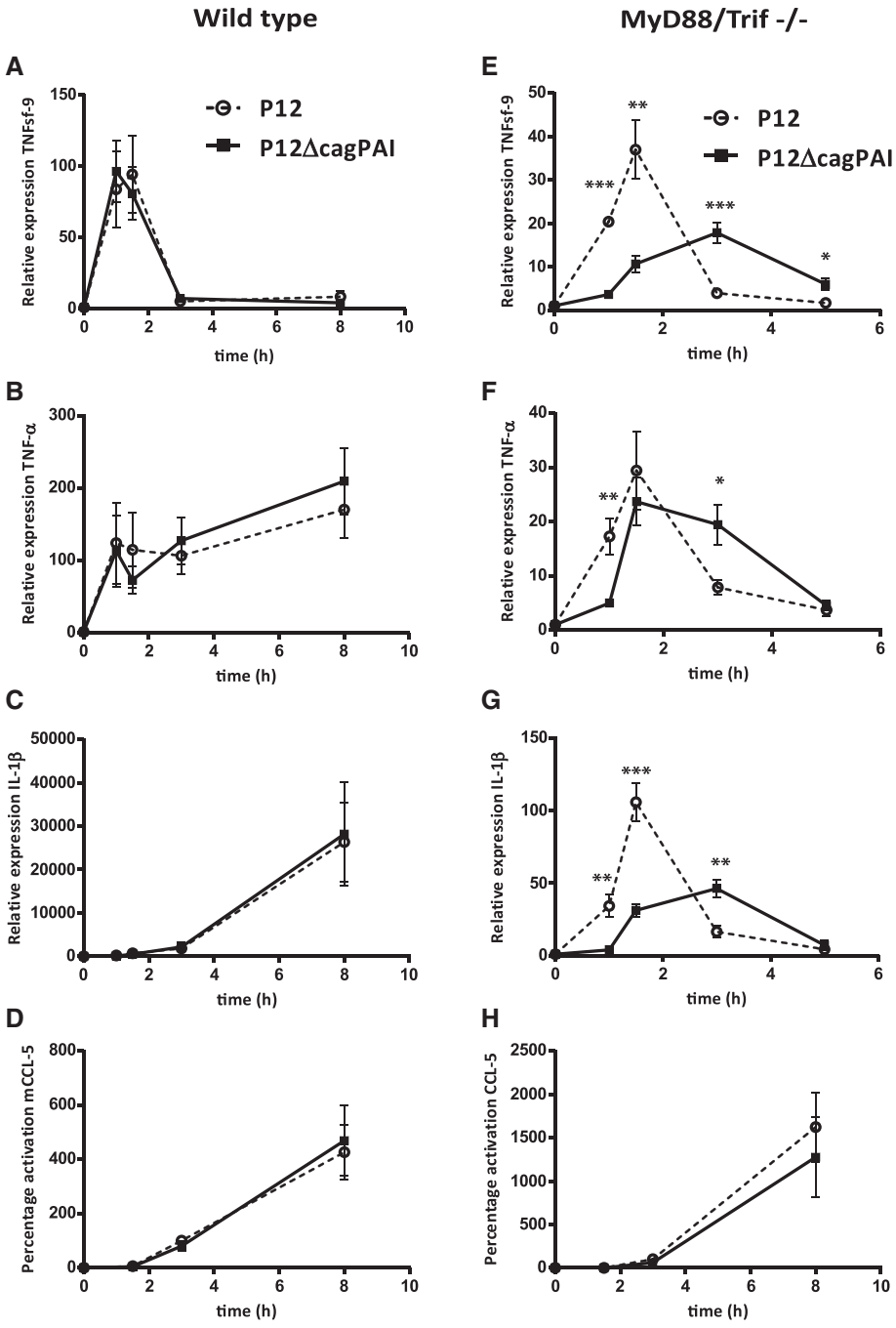

Fig. 1. MyD88/Trif$^{-/-}$ but not wt macrophages differentiate between P12 and P12Δ*cagPAI* infection through different kinetic behaviour for group I (ARE-containing) early response genes. Wild-type and MyD88/Trif$^{-/-}$ BMMs were infected with either wt *Helicobacter pylori* P12 or P12Δ*cagPAI* and the expression levels of selected pro-inflammatory genes examined by qRT-PCR over the course of up to 8 h. In wt BMMs, there was no difference in expression of (A) TNFsf9, (B) TNF-α and (C) IL-1β between the two strains; CCL-5 (D) served as a control. (E)–(G) By contrast, in MyD88/Trif$^{-/-}$ BMMs, the expression of all three genes (E) TNFsf9, (F) TNF-α and (G) IL-1β in response to wt P12 exhibited early gene kinetics. In addition, the kinetics are significantly slower and less stable in response to P12Δ*cagPAI*. There was no difference in the expected kinetics for the ARE-negative control gene mCCL-5 (H). Experiments were performed in triplicate reactions; bars represent mean ± SEM of at least three biologically independent replicates. $^{*}P < 0.05$, $^{**}P < 0.01$, $^{***}P < 0.001$, Student's *t*-test.

for 3 h, followed by gene expression analysis via microarray. Supporting Information Fig. S3 presents a heat map of gene expression changes in P12-infected wt, MyD88/Trif$^{-/-}$ and MyD88/Trif/Rip2$^{-/-}$ BMMs with a >10-fold change compared to mock infection in at least one of the groups. No substantial differences were observed between infected MyD88/Trif$^{-/-}$ and MyD88/Trif/Rip2$^{-/-}$ BMMs, but substantial differences were evident when comparing the mutant BMMs to wt. From this analysis, it appears that neither Rip2, nor, by consequence, NOD1 or NOD2 play significant roles in *H. pylori* detection by BMMs.

Early regulation is contact dependent and partially nuclear factor-κB dependent

To examine the mechanism of up-regulation of the early response genes TNFsf9, IL-1β and TNF-α, we first tested whether this effect was dependent on direct contact of *H. pylori* with the host cell or on phagocytic uptake of the bacterium. To this end, we used bafilomycin A1 (BafA1),

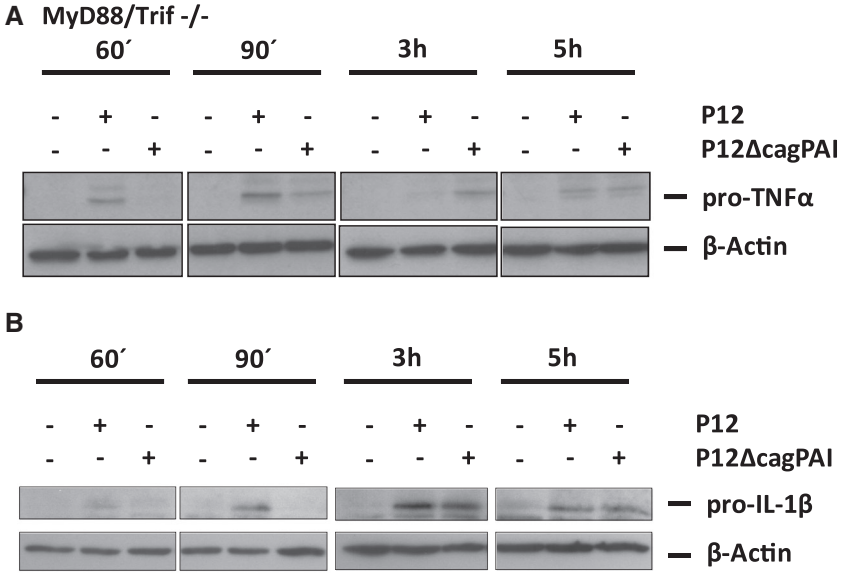

Fig. 2. Differential up-regulation of the early response genes TNF-α and IL-1β in MyD88/Trif$^{-/-}$ is also reflected on protein level. Protein expression of pro-TNF-α (A) and pro-IL-1β (B) was followed from 60 min to 5 h in P12 and P12Δ*cagPAI*-infected MyD88/Trif$^{-/-}$ BMMs. Western blots were performed with three biological replicates using β-actin as endogenous control, shown here is a representative image for both genes.

an inhibitor of phagosomal maturation that blocks the host cell proton pump. When we pre-treated MyD88/Trif$^{-/-}$ BMMs with BafA1 1 h prior to infection with P12 wt for 60 min, we could not detect any difference in RNA expression of TNF-α and TNFsf9 and only a moderate, but non-significant, decrease of IL-1β (Fig. 3A–C). Moreover, pre-treating MyD88/Trif$^{-/-}$ BMMs with the proteasome inhibitor MG-132 to inhibit the NF-κB pathway, we observed a strong decrease in IL-1β and TNFsf9 expression during wt P12 infection, but no reduction in the expression of TNF-α (Fig. 3A–C). Thus, these results further underscore that the response depends on direct contact between *H. pylori* and macrophages, independently of phagosomal maturation. Moreover, while IL-1β and TNFsf9 expression seems to be critically dependent on NF-κB activity, TNF-α activation seems to require an independent component.

CagT4SS but not its CagA effector protein is necessary for virulence discrimination

To assess which feature of the cagPAI is involved in the signalling process, we first used Western blotting to test if CagA is translocated and phosphorylated in mouse BMMs. Using antibodies against phospho-tyrosine motifs and CagA, we detected a major band at ~40 kDa (Supporting Information Fig. S4), indicating that phosphorylated CagA is effectively translocated but fragmented in these BMMs, consistent with our previous observations (Moese *et al*., 2001). As we wanted to know whether CagA influences the expression pattern of the early response genes TNF-α, IL-1β and TNFsf9 in anergic macrophages, we infected MyD88/Trif$^{-/-}$ BMMs with P12 wt, P12Δ*cagPAI*, P12Δ*cagA* or the cagL deletion mutant P12Δ*cagL*. CagL is a structural element of the CagT4SS

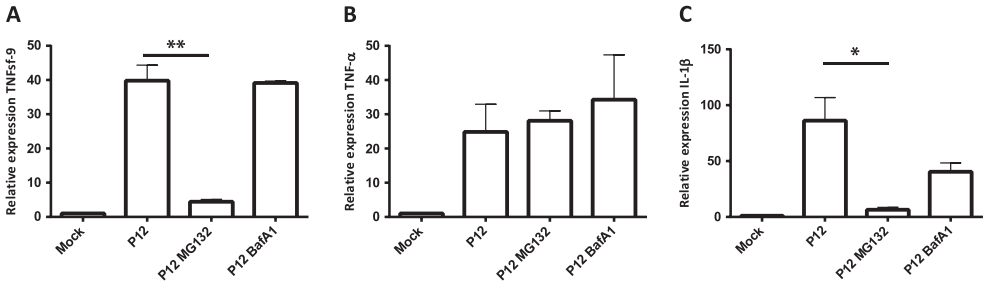

Fig. 3. Early response is contact dependent and partially NF-κB dependent. MyD88/Trif$^{-/-}$ BMMs were infected with wt *Helicobacter pylori* P12 for 60 min in the presence of the phagosomal maturation inhibitor BafA1, (100nM), or the proteasome inhibitor MG132 (50 μM) from 1 h prior to infection. Expression of (A) TNFsf9, (B) TNF-α and (C) IL-1β was analysed by qRT-PCR. Experiments were performed in triplicate reactions; bars represent mean ± SEM of at least three biologically independent replicates.*$P < 0.05$, **$P < 0.01$, Student's *t*-test.

that binds to host cell integrins (Kwok *et al*., 2007; Jimenez-Soto *et al*., 2009). P12Δ*cagA* induced an early response of the selected genes similar to wt P12 (Fig. 4A–C). In contrast, infection with P12Δ*cagL* resulted in much slower kinetics similar to P12Δ*cagPAI* infection. Hence, we conclude that cagPAI detection in MyD88/Trif$^{-/-}$ macrophages occurs via the T4SS and not via the CagA effector protein.

Discussion

Several reports have demonstrated a strong connection between the presence of the cagPAI-encoded T4SS in *H. pylori* and an increased inflammation and pathogenesis (Kusters *et al*., 2006). This implicates a mechanism of molecular recognition of this virulence determinant in host cells. Using a murine model, we demonstrate here the specific detection of the cagT4SS; however, this mechanism is masked in wild type BMMs, which are TLR signalling proficient. Our results indicate a selective recognition of highly virulent versus less virulent (cagPAI-negative) *H. pylori* strains by anergic macrophages of the human-infected mucosa through a TLR-independent pathway.

Using MyD88/Trif$^{-/-}$ BMMs, we observed a strong reduction in the expression of ~70% of the genes that are up-regulated upon *H. pylori* infection of wt BMMs. These data are in congruence with Rad *et al*. (2007), who obtained similar numbers using MyD88$^{-/-}$ bone marrow dendritic cells (DCs) in a cagPAI negative *H. pylori* infection model. It also indicates that in contrast to previous reports (Moran *et al*., 1997; Andersen-Nissen *et al*., 2005), *H. pylori* expresses potent ligands capable of inducing TLR signalling. Franchi *et al*. (2012) proposed that differentiation of pathogens by anergic macrophages takes place on the level of the inflammasome. The same group also suggested that recognition of *H. pylori* and pro-IL-1β expression depends on TLR-2 and NOD-2 (Kim *et al*., 2013). We demonstrate here that differentiation already occurs at the transcriptional level but only in macrophages that lack TLR receptor signalling, irrespective of the presence of NOD receptors.

In MyD88/Trif$^{-/-}$ macrophages, numerous genes exhibited different expression kinetics for cagPAI positive and negative *H. pylori*, and almost all of them contained ARE sequences. Differential activation of macrophages in response to different pro-inflammatory stimuli via mRNA stabilization has also been observed by Hao and Baltimore (2009), but how exactly gene expression kinetics is translated into an appropriate immune response is not yet clear. In wt BMMs, these ARE-containing genes exhibited early, intermediate or late gene kinetics (Hao and Baltimore, 2009). In MyD88/Trif$^{-/-}$ BMMs, IL-1β and TNF-α switched from late/intermediate to early gene kinetics if the

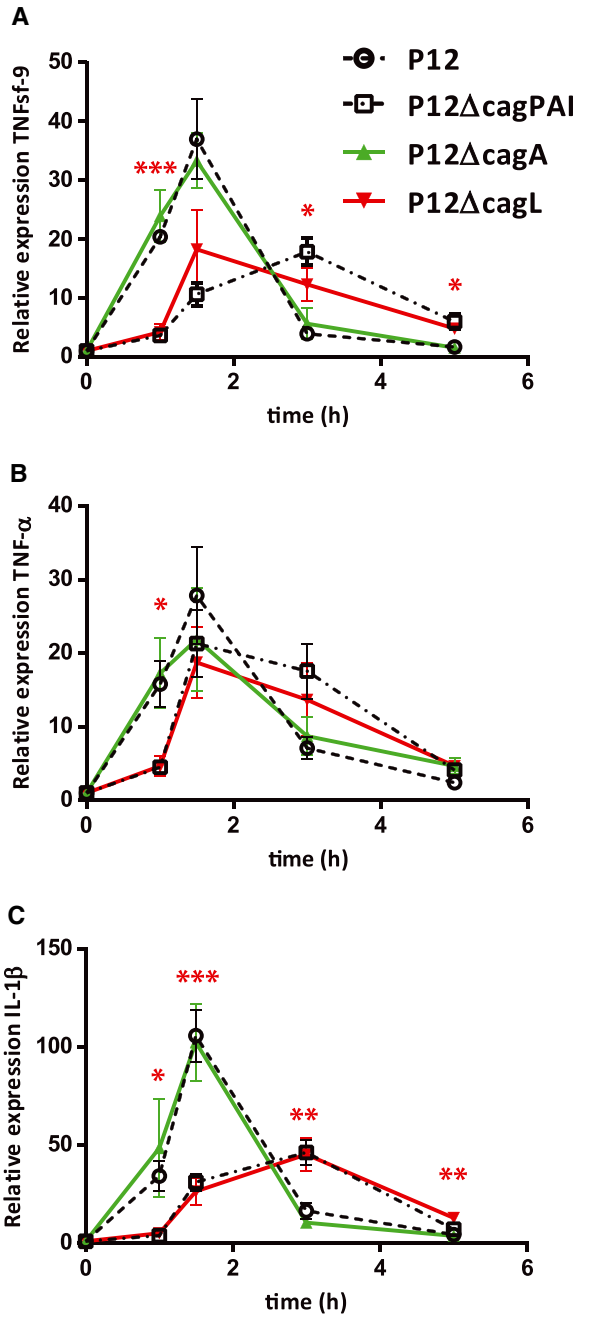

Fig. 4. MyD88/Trif$^{-/-}$ macrophages differentiate between cagPAI positive and negative strains through recognition of the T4SS but not CagA. Anergic MyD88/Trif$^{-/-}$ BMMs were infected (MOI 50) with wt *Helicobacter pylori* P12, P12Δ*cagPAI*, P12Δ*cagA* or P12Δ*cagL*, and the expression levels of selected pro-inflammatory genes were examined by qRT-PCR over the course of 5 h. (A) TNFsf9, (B) TNF-α and (C) IL-1β all showed early gene expression kinetics in response to P12 and P12Δ*cagA*. Expression kinetics were significantly delayed and reduced in response to P12Δ*cagPAI* and P12Δ*cagL*. Experiments were performed in triplicate reactions; bars represent mean ± SEM of at least three biologically independent replicates. Asterisks indicate significance levels of Student's *t*-test performed between P12 and P12Δ*cagL*. $^{*}P < 0.05$, $^{**}P < 0.01$.

bacteria harboured the cagPAI. Hao and Baltimore (2009) also observed early response gene kinetics for IL-1β and TNF-α in response to TNF-α stimulation; however, mRNA stability for these two genes was increased when LPS was used as the inducer. In our experiments, the phenotypes seen after *H. pylori* cagPAI detection in MyD88/Trif$^{-/-}$ macrophages are reminiscent of those seen after TNF-α treatment. It is likely that the kinetic behaviour of particular genes is influenced not only by its ARE content but also several other layers of control, e.g. RNA splicing (Hao and Baltimore, 2013), and the availability of transcription factor binding sites, e.g. for the immune modulator NF-κB (Iwanaszko *et al.*, 2012).

Stabilization of ARE-containing genes has been observed as an effect of LPS (Hao and Baltimore, 2009). LPS may act via TLR-4 to destabilize the interaction between ARE-containing mRNAs with the RNA binding protein tristetraprolin (Hitti *et al.*, 2006), which is responsible for degrading specific ARE-containing mRNAs in BMMs (Kratochvill *et al.*, 2011). Many of these were also identified in our list of cagPAI-regulated genes. In wt macrophages, therefore, TLRs appear to mask recognition of the cagPAI. While our findings reveal evidence of a virulence discrimination mechanism, the underlying signalling routes require further investigation. It is possible that a similar mechanism also occurs in gastric epithelial cells, which only react to cagPAI+ strains but not to TLR ligands with an inflammatory response (Belogolova *et al.*, 2013). There is an ongoing debate about the role of NOD receptors during this process (Viala *et al.*, 2004; Backert and Naumann, 2010). It has been suggested that NOD1 induces NF-κB signalling in gastric epithelial cells via detection of T4SS-translocated peptidoglycan (Viala *et al.*, 2004). We can exclude that the adaptor protein of NOD1 and NOD2, Rip2, plays a crucial role in our model, because gene expression in MyD88/Trif/Rip2$^{-/-}$ and MyD88/Trif$^{-/-}$ BMMs was similar. We can also exclude a role of CagA effector protein in recognition by macrophages, because the CagA mutant showed the same gene expression kinetics as wt P12. Similarly, previous work excluded a role for CagA during induction of an innate immune response in gastric epithelial cells (Schweitzer *et al.*, 2010).

Two possibilities may explain our data as well as other published work. CagL protein was necessary for detection of virulent strains in our model and represents an excellent candidate for direct recognition in anergic macrophages via integrin receptors. Gorrell *et al.* (2013) also reported direct CagL-mediated activation of IL-8 in gastric epithelial cells. However, there is an ongoing debate on whether CagL is a direct integrin binding partner located on the tip of the CagT4SS or only important for the formation of the cagT4SS machinery (Kwok *et al.*, 2007; Shaffer *et al.*, 2011), and we cannot rule out that there is an additional effector molecule that is translocated via the CagT4SS.

Macrophages of the gastro-intestinal tract have been shown to be unresponsive to TLR ligands (Smith *et al.*, 2011); thus, virulence discrimination by MyD88/Trif$^{-/-}$ macrophages as observed here might also play a role in sensing the pathogenic potential of other human bacterial species, such as the T4SS or T3SS producing pathogens enteropathogenic *E. coli* and *B. pertussis*. As such, it may turn out to be crucial for maintaining a healthy gut microbiota.

Experimental procedures

Mice were maintained according to the German Animal Welfare Act (TierSchG), German Laboratory Animal Directive (TierSchVersV) and European Directive 86/609/EEC for the protection of animals used for experimental and scientific purposes and kept under specific pathogen-free conditions according to Federation of European Laboratory Animal Science Association (felasa) recommendations. The protocol for sacrification and preparation of organs was approved by the Committee for Animal Experiments of the Berlin State Office for Health and Social Affairs (LAGeSo), permission number T0087/08.

Mice

MyD88/Trif$^{-/-}$ mice were a kind gift from the Faculty of Veterinary Medicine, Technical University, Munich and have been described previously (Koch *et al.*, 2012). Rip2$^{-/-}$ (B6.129S1-Ripk2tm1Flv/J) mice were purchased from Jackson Laboratories. Mice deficient in MyD88/Trif/Rip2$^{-/-}$ were generated by crossing MyD88/Trif$^{-/-}$ mice with Rip2$^{-/-}$ mice as described (Koch *et al.*, 2012). Because the MyD88/Trif/Rip2$^{-/-}$ triple knockout could not be bred homozygously, they were bred as MyD88$^{-/-}$/Trif$^{+/-}$/Rip2$^{-/-}$, and only the triple knockout was used for experiments. As control, wt BMMs were isolated from C57BL/6J mice.

Generation of bone marrow-derived macrophages

Bone marrow-derived macrophages were generated according to a standard protocol (Collins *et al.*, 1997). Adult mice (>8 weeks) were sacrificed by cervical dislocation and the femur and tibia removed. Monocytic precursors were isolated by opening the ends of the bone and removing the bone marrow with a syringe containing RPMI medium. Bone marrow was pressed through a cell strainer (70 μm, BD Falcon) and washed three times with phosphate-buffered saline (PBS) (Gibco). The pellet was resuspended in RPMI-1640 medium (Gibco) and plated in 10 cm dishes in RPMI medium containing 10% fetal calf serum (FCS) (heat-inactivated, hi) and 30% supernatant of L929 cells as source of macrophage colony-stimulating factor (M-CSF). After 7 days, culture cells were washed

twice with PBS and replated overnight in RPMI medium containing 10% hi FCS and 10% L929 supernatant.

Bacterial strains

Helicobacter pylori P12 (strain collection number 243) and its isogenic mutants P12Δ*cagPAI* (number P387), P12Δ*cagL* (number P454) and P12Δ*cagA* (number P378) as described previously (Koch *et al*., 2012) were plated from glycerol stock and grown on gonococcal agar plates containing 10% horse serum, 10 μg ml^{-1} vancomycin, 1 μg ml^{-1} nystatin and 5 μg ml^{-1} trimethoprim. They were kept under micro-aerophilic conditions (5% CO_2 and 4% O_2) and replated after 3 days. Following replating after 1 day (maximum of three times), bacteria were ready for infection.

Infection experiments

Bacteria were washed twice with PBS prior to infection and added in a defined volume of PBS. All experiments were carried out at MOI 50. To determine MOI, a calibration curve was generated for the bacteria by measuring optical density at 550 nm (OD550). Mock infection was defined as the non-infected control using the same volume of PBS. Before infection, medium was exchanged to RPMI medium containing no additional supplements. The number of BMMs was determined by optical confluency using a standard curve. For the inhibitor studies, the BMMs were pretreated with the inhibitors bafilomycin A1 (100 nM) and MG-132 (50 μM, both from Sigma) 1 h prior to infection. Inhibitors were dissolved in dimethyl sulfoxide (DMSO), and the same volume of DMSO was used for the infected and mock control.

The q reverse transcription polymerase chain reaction experiments

Total RNA was isolated by the Trizol (Invitrogen) method following manufacturer's protocol. For detection of mRNAs, the SYBR green method in one-step was applied by using the RNA-to-CT assay according to the manufacturer's protocol (Applied Biosystems). Approximately 10 ng of the total RNA was used for each reaction. Relative expression levels were determined applying the ΔΔCT method using β-actin as endogenous control and normalized to mock infected cells unless stated otherwise. Primer sequences are listed in Table S1. For each primer pair, a standard curve was generated to determine efficiency with at least three different concentrations of mRNA. An efficiency of 3.3 (±10%) for 10-fold concentration change was accepted for a primer pair to be used for ΔΔCT method. Efficiencies and correlation coefficients are shown in the primer list (Table S1).

Western blot experiments

For Western blotting, samples were directly harvested in Lämmli buffer. Ten percent of sodium dodecyl sulfate polyacrylamide gel electrophoresis gels were used for discontinuous gel electrophoresis followed by semi-dry blotting onto polyvinylidene difluoride membrane. The membrane was blocked with 3% bovine serum albumin in Tris-buffered saline buffer containing 0.1% Tween-20 (TBS-T) (blocking buffer). Antibodies against β-actin (A5441, Sigma), TNF-α (CS3707, cell signalling), IL-1β (Ab9722, Abcam), CagA bK20 (sc-48128) and p-Tyr (sc-7020, both Santa Cruz) were diluted in blocking buffer and incubated overnight at 4 °C. Primary antibody was removed, and the membrane was washed for 1 h at room temperature (RT) then incubated with secondary antibody for 1 h at RT followed by three washes with TBS-T. Enhanced chemiluminescence (ECL) solution (Amersham) was added to the membrane and signal detected by Hyperfilm ECL (Amersham), and scanned, and images prepared with Adobe Photoshop.

Microarray analysis

Microarray experiments were performed as dual-colour hybridizations. To compensate for dye-specific effects, independent dye-reversal colour swap was applied. Quality control and quantification of total RNA were assessed using an Agilent 2100 Bioanalyzer (Agilent Technologies) and a NanoDrop 1000 ultraviolet-visible spectrophotometer (Kisker). RNA labelling was performed with the dual-colour quick-amp labelling kit (Agilent Technologies). mRNA was reverse transcribed and amplified using an oligo-dT-T7 promoter primer, and resulting cRNA was labelled with cyanine 3-CTP or cyanine 5-CTP. After precipitation, purification and quantification, 1.25 μg of each labelled cRNA was fragmented and hybridized to whole-mouse genome 4 × 44 k multipack microarrays (AMADID 014868) according to supplier's protocol (Agilent Technologies). Scanning of microarrays was performed with 5 μm resolution using a G2565CA high-resolution laser microarray scanner (Agilent Technologies) with extended dynamic range. Raw microarray image data were analysed with image analysis/feature extraction software G2567AA v. A.10.5.1 (Agilent Technologies) using default settings and the GE2_105_Jan09 protocol. Extracted MAGE-ML files were analysed further with Rosetta Resolver Biosoftware, Build 7.2.2 SP1.31 (Rosetta Biosoftware). Ratio profiles comprising single hybridizations were combined in an error-weighted fashion to create ratio experiments. Unless stated otherwise, a 1.5-fold change expression cut-off for ratio experiments was applied together with anti-correlation of ratio profiles, rendering the microarray analysis highly significant ($P < 0.01$), robust and reproducible. Only genes with a Refseq accession (NM_…) were taken for further analysis. The heat maps were generated with the Rosetta Resolver software using a fold change cut-off of >10-fold in at least one of the infected BMMs compared to mock

infection. Microarray data presented in this paper have been deposited in the National Center for Biotechnology Information Gene Expression Omnibus (GEO; http://www.ncbi.nlm.nih.gov/geo/) and are accessible through GEO series accession number GSE56791.

Statistical analysis

For testing significance of differentially up-regulated genes, an unpaired homoscedastic two-sided Student's *t*-test was performed. In rare cases of extreme values, a maximum of one outlier was removed using Grubbs' test (GraphPad Prism). For testing enrichment of ARE-containing genes, all genes in Table 1 were evaluated for presence of pentameric AU-rich elements using the ARESite algorithm (Gruber *et al*., 2011) and checking significance compared to all genes by χ^2 test.

Acknowledgements

We would like to thank Kirstin Hoffmann, Ina Wagner and the members of the MPI experimental animal core facility for excellent technical assistance and Rike Zietlow for editing the manuscript.

This work was supported by the DFG (through SFB633 project B12 to TFM).

Author contributions

M. K. designed, performed and analysed experiments; H. J .M. performed and analysed the microarray experiments; M. K. and T. F. M. conceived the project and wrote the manuscript; T. F. M. supervised the project.

Conflict of interest

The authors declare no commercial or financial conflict of interest.

References

Andersen-Nissen, E., Smith, K.D., Strobe, K.L., Barrett, S.L., Cookson, B.T., Logan, S.M. and Aderem, A. (2005) Evasion of toll-like receptor 5 by flagellated bacteria. *Proc Natl Acad Sci U S A* **102**:9247–9252.

Arnold, I.C., Lee, J.Y., Amieva, M.R., *et al*. (2011) Tolerance rather than immunity protects from *Helicobacter pylori*-induced gastric preneoplasia. *Gastroenterology* **140**: 199–209.

Backert, S., and Naumann, M. (2010) What a disorder: proinflammatory signaling pathways induced by *Helicobacter pylori*. *Trends Microbiol* **18**: 479–486.

Bartfeld, S., Hess, S., Bauer, B., *et al*. (2010) High-throughput and single-cell imaging of NF-kappaB oscillations using monoclonal cell lines. *BMC Cell Biol* **11**: 21.

Belogolova, E., Bauer, B., Pompaiah, M., *et al*. (2013) *Helicobacter pylori* outer membrane protein HopQ identified as a novel T4SS-associated virulence factor. *Cell Microbiol* **15**:1896–1912.

Chaput, C., Ecobichon, C., Cayet, N., *et al*. (2006) Role of AmiA in the morphological transition of *Helicobacter pylori* and in immune escape. *PLoS Pathog* **2**:e97.

Collins, H.L., Schaible, U.E., Ernst, J.D., and Russell, D.G. (1997) Transfer of phagocytosed particles to the parasitophorous vacuole of *Leishmania mexicana* is a transient phenomenon preceding the acquisition of annexin I by the phagosome. *J Cell Sci* **110**(Pt 2): 191–200.

Engler, D.B., Leonardi, I., Hartung, M.L., *et al*. (2015) *Helicobacter pylori*-specific protection against inflammatory bowel disease requires the NLRP3 inflammasome and IL-18. *Inflamm Bowel Dis* **21**: 854–861.

Franchi, L., Kamada, N., Nakamura, Y., *et al*. (2012) NLRC4-driven production of IL-1beta discriminates between pathogenic and commensal bacteria and promotes host intestinal defense. *Nat Immunol* **13**: 449–456.

Gorrell, R.J., Guan, J., Xin, Y., Tafreshi, M.A., Hutton, M.L., McGuckin, M.A. *et al*. (2013) A novel NOD1- and CagA-independent pathway of interleukin-8 induction mediated by the *Helicobacter pylori* type IV secretion system. *Cell Microbiol*. **15**: 554–570

Gruber, A.R., Fallmann, J., Kratochvill, F., Kovarik, P., and Hofacker, I.L. (2011) AREsite: a database for the comprehensive investigation of AU-rich elements. *Nucleic Acids Res* **39**: D66–D69.

Hao, S., and Baltimore, D. (2009) The stability of mRNA influences the temporal order of the induction of genes encoding inflammatory molecules. *Nat Immunol* **10**: 281–288.

Hao, S., and Baltimore, D. (2013) RNA splicing regulates the temporal order of TNF-induced gene expression. *Proc Natl Acad Sci U S A* **110**: 11934–11939.

Hitti, E., Iakovleva, T., Brook, M., *et al*. (2006) Mitogen-activated protein kinase-activated protein kinase 2 regulates tumor necrosis factor mRNA stability and translation mainly by altering tristetraprolin expression, stability, and binding to adenine/uridine-rich element. *Mol Cell Biol* **26**: 2399–2407.

Iwanaszko, M., Brasier, A.R., and Kimmel, M. (2012) The dependence of expression of NF-κB-dependent genes: statistics and evolutionary conservation of control sequences in the promoter and in the 3'UTR. *BMC Genomics* **13**: 182.

Jimenez-Soto, L.F., Kutter, S., Sewald, X., *et al*. (2009) *Helicobacter pylori* type IV secretion apparatus exploits beta1 integrin in a novel RGD-independent manner. *PLoS Pathog* **5**: e1000684.

Kawai, T., and Akira, S. (2011) Toll-like receptors and their crosstalk with other innate receptors in infection and immunity. *Immunity* **34**: 637–650.

Kim, D.J., Park, J.H., Franchi, L., Backert, S., and Nunez, G. (2013) The Cag pathogenicity island and interaction between TLR2/NOD2 and NLRP3 regulate IL-1beta production in *Helicobacter pylori* infected dendritic cells. *Eur J Immunol* **43**: 2650–2658.

Koch, M., Mollenkopf, H.J., Klemm, U., and Meyer, T.F. (2012) Induction of microRNA-155 is TLR- and type IV secretion system-dependent in macrophages and inhibits DNA-damage induced apoptosis. *Proc Natl Acad Sci U S A* **109**: E1153–E1162.

Kratochvill, F., Machacek, C., Vogl, C., *et al*. (2011) Tristetraprolin-driven regulatory circuit controls quality and

timing of mRNA decay in inflammation. *Mol Syst Biol* **7**: 560.
Kusters, J.G., van Vliet, A.H., and Kuipers, E.J. (2006) Pathogenesis of *Helicobacter pylori* infection. *Clin Microbiol Rev* **19**: 449–490.
Kwok, T., Zabler, D., Urman, S., *et al*. (2007) *Helicobacter* exploits integrin for type IV secretion and kinase activation. *Nature* **449**: 862–866.
Moese, S., Selbach, M., Zimny-Arndt, U., Jungblut, P.R., Meyer, T.F., and Backert, S. (2001) Identification of a tyrosine-phosphorylated 35 kDa carboxy-terminal fragment (p35CagA) of the *Helicobacter pylori* CagA protein in phagocytic cells: processing or breakage? *Proteomics* **1**: 618–629.
Moran, A.P., Lindner, B., and Walsh, E.J. (1997) Structural characterization of the lipid A component of *Helicobacter pylori* rough- and smooth-form lipopolysaccharides. *J Bacteriol* **179**: 6453–6463.
Mowat, A.M. and Bain, C.C. (2011) Mucosal macrophages in intestinal homeostasis and inflammation. *J Innate Immun* **3**: 550–564.
Oertli, M., Sundquist, M., Hitzler, I., Engler, D.B., Arnold, I.C., Reuter, S., *et al*. (2012) DC-derived IL-18 drives Treg differentiation, murine *Helicobacter pylori*-specific immune tolerance, and asthma protection. *J Clin Invest* **122**: 1082–1096.
Rad, R., Brenner, L., Krug, A., *et al*. (2007) Toll-like receptor-dependent activation of antigen-presenting cells affects adaptive immunity to *Helicobacter pylori*. *Gastroenterology* **133**: 150–63.e3.
Rad, R., Ballhorn, W., Voland, P., *et al*. (2009) Extracellular and intracellular pattern recognition receptors cooperate in the recognition of *Helicobacter pylori*. *Gastroenterology* **136**: 2247–2257.
Schwanhausser, B., Busse, D., Li, N., *et al*. (2011) Global quantification of mammalian gene expression control. *Nature* **473**: 337–342.
Schweitzer, K., Sokolova, O., Bozko, P.M., and Naumann, M. (2010) *Helicobacter pylori* induces NF-κB independent of CagA. *EMBO Rep* **11**: 10–11; author reply 1-2.
Shaffer, C.L., Gaddy, J.A., Loh, J.T., *et al*. (2011) *Helicobacter pylori* exploits a unique repertoire of type IV secretion system components for pilus assembly at the bacteria-host cell interface. *PLoS Pathog* **7**: e1002237.
Smith, P.D., Smythies, L.E., Shen, R., Greenwell-Wild, T., Gliozzi, M., and Wahl, S.M. (2011) Intestinal macrophages and response to microbial encroachment. *Mucosal Immunol* **4**: 31–42.
Smythies, L.E., Shen, R., Bimczok, D., Novak, L., Clements, R.H. Eckhoff, D.E., *et al*. (2010) Inflammation anergy in human intestinal macrophages is due to Smad-induced IkappaBalpha expression and NF-kappaB inactivation. *J Biol Chem* **285**: 19593–19604.
Viala, J., Chaput, C., Boneca, I.G., *et al*. (2004) Nod1 responds to peptidoglycan delivered by the *Helicobacter pylori* cag pathogenicity island. *Nat Immunol* **5**: 1166–1174.
Walter, J. and Ley, R. (2011) The human gut microbiome: ecology and recent evolutionary changes. *Annu Rev Microbiol* **65**: 411–429.
Yamaoka, Y., Kita, M., Kodama, T., Sawai, N., Kashima, K., and Imanishi, J. (1997) Induction of various cytokines and development of severe mucosal inflammation by cagA gene positive *Helicobacter pylori* strains. *Gut* **41**: 442–451.

Supporting information

Additional Supporting Information may be found in the online version of this article at the publisher's web-site:

Table S1. Primers used for qRT-PCR.
Fig. S1. TLR-dependence of genes that were found to be strongly (> 10-fold) induced by H. pylori in wt BMMs.
Fig. S2. Unspecific effects via differences in motility can be excluded.
Fig. S3. The adaptor protein of the NOD like receptors NOD1 and NOD2, Rip2, does not play a significant role in the detection of H. pylori in BMMs.
Fig. S4. CagA gets translocated into BMMs and is processed.